J Mater Sci (2007) 42:9308–9315
DOI 10.1007/s10853-007-1883-4

Analysis of stress-induced phase transformations in elastoplastic materials with strain-softening behavior under plane shear

Y. T. Zhang · T. Ao · J. F. Xu

Received: 21 February 2007 / Accepted: 25 May 2007 / Published online: 28 July 2007

Abstract Possible two-phase piecewise-homogeneous deformations in elastoplastic materials with strain-softening behavior under plane shear are analyzed. Discontinuities of stress and deformation gradient across interfaces between phases are considered and continuity of traction and displacement across interfaces and the Maxwell relation is imposed. The governing equations are obtained. The analysis is reduced to finding a minimum value of the loading at which governing equations have a unique, real, physically acceptable solution. It is found that for a plate with constant thickness under plane shear two-phase piecewise-homogeneous deformations are possible, and the Maxwell stress, the stresses and strains in both phases, the jumps of stress and deformation gradient across interfaces and the inclination angle of the localized deformed band can all be determined. As an illustration, a NiTi alloy plate under plane shear is numerically analyzed. The inclination angle of the martensite band is predicted to be 90°, and this predicted value can be applied to explain why no locally deformed spiral martensite band was observed in experiments on thin-walled NiTi alloy tubes under torsion.

Introduction

Stress-induced phase transformations in strips and thin-walled tubes under uniaxial loading (tension/compression) were widely observed in experiments, see, e.g., Wattrisse et al. [1], Corona et al. [2], Shaw and Kyriakides [3] and Sun and Li [4], where inclined and locally deformed bands, the Lüders bands or martensite bands (M-bands), were observed, and stress–strain response curves with peak stress, sudden dropping and the Maxwell stress plateau were also measured.

In order to simulate the stress-induced phase transformations from austenite to martensite in NiTi alloy strips under uniaxial tension observed in experiments, Shaw and Kyriakides [5] modeled the NiTi alloy as elastoplastic solids with strain-softening behavior, and the value of the lower yield stress of NiTi alloy, which cannot be measured in experiments, were approximately assumed. The strip was discretized with three-dimensional, 20-nodes (quadratic), brick elements, and a geometric imperfection (small indentation) in a side of the strip was introduced artificially to ensure that localized deformation could initiate from there. The localized deformation in the NiTi alloy strip was numerically simulated and was used to simulate the initiation and propagation of phase transformation from austenite to martensite. Similar finite element methods were also used by Kyriakides and Miller [6], Corona et al. [2] and Sun et al. [7] to simulate the initiation and propagation of the Lüders band in fine grained steel strips under uniaxial tension/compression.

In the simulations above, however, discontinuities of stress and deformation gradient across the quite sharp interfaces between two phases was not considered; and, more crucially, the Maxwell relation which is necessary for phase transformations was not imposed.

Recently, based on the theory of phase transformations Zhang et al. [8] suggested a method to determine theoretically the value of the lower yield stress of materials with strain-softening behavior. An analytical investigation of stress-induced phase transformations in elastoplastic

Y. T. Zhang (✉) · T. Ao · J. F. Xu
Department of Mechanics, Tianjin University, Tianjin 300072, China
e-mail: ytzhang@tju.edu.cn

materials with strain-softening behavior under uniaxial compression was also provided. It was shown that two-phase piecewise-homogeneous deformations can coexist in materials with strain-softening behavior under uniaxial compression, and the predicted values of the Maxwell stress, the inclination angle of the Lüders band and the kink angle of the strip were in reasonable agreement with the experimental measurements by Corona et al. [2].

In the present paper, an analytical study of stress-induced phase transformations in elastoplastic materials with strain-softening behavior under plane shear is carried out. Unlike the experiments under uniaxial loading, experiments on the stress-induced phase transformations under shear are seldom reported in the literature. A paper about experiments on NiTi alloy thin-walled tubes under tension can be found, see Sun and Li [4]. It was observed that under tension–torsion combined loading with an increasing shear/tension stress ratio, there was a gradual change in the deformation mode from localization and propagation of the M-bands (under pure tension) to the homogeneous deformation of the M-bands (under pure shear). In other words, no localized deformed M-bands in thin-walled NiTi alloy tubes under torsion were observed. The predicted result in this paper will give a good explanation for the experimental observation.

The rest of this paper is organized as follows. After the possible two-phase piecewise-homogeneous deformation of a plate under pure shear is described in the following section, analysis of two-phase equilibrium under plane shear is provided in Section "Analysis of two-phase equilibrium under plane shear". In Section "Numerical illustration", the stress–strain response curve of NiTi alloy under uniaxial tension given by Shaw and Kyriakides [5] is used to calibrate the three-dimensional elastoplastic model proposed by Rice and Hill, and phase transformations in NiTi alloy plates under pure shear are analyzed. In Section "Thin-walled NiTi alloy tube under torsion" the predicted value of inclination angle of the martensite band is used to explain why no locally deformed spiral M-bands were observed in experiments on thin-walled NiTi alloy tubes under torsion. In the final section we summarize our main results.

Two-phase piecewise-homogeneous deformation of a plate under pure shear in the $X_1\,OX_2$ plane

A common Cartesian coordinate system for both the reference and deformed configurations is used in the present paper. A typical material particle of plates whose position vector in the reference configuration is denoted by (X_1, X_2, X_3) has a position vector (x_1, x_2, x_3) in the deformed configuration. The top view of a plate with constant thickness under the shear in the $X_1\,OX_2$ plane with possible two-phase piecewise-homogeneous deformations is sketched in Fig. 1, where the two phases are denoted by '–' and '+', respectively. The '–' phase is the phase of materials under elastic deformation, and the '+' phase is a possible localized deformed band. The unit vector that is normal to the interface between the two phases in the reference configuration and points from the '+' phase into the '–' phase is denoted by $\boldsymbol{N} = [N_1, N_2, N_3]^T$, and the inclination angle of the possible '+' band to the X_2-axis is denoted by α.

We consider the following shear deformation in the $X_1\,OX_2$ plane in the '–' phase whose deformation gradient tensor, denoted by $\boldsymbol{F}^-$, can be written as

$$\boldsymbol{F}^- = \begin{bmatrix} 1 & \omega & 0 \\ 0 & \lambda_2 & 0 \\ 0 & 0 & 1 \end{bmatrix}, \tag{1}$$

where ω is the amount of shear as shown in Fig. 1, $\lambda_2 = \sqrt{1-\omega^2}$ is the stretch in the X_2-axis direction, and the superscript/subscript "+" and "–" signify evaluation inside the "+" phase or the "–" phase, respectively. When there is no "+" or "–" superscript/subscript attached to a field variable evaluated at interface, it means that the variable can be evaluated on either side of the interface.

By Eq. 1 the corresponding Green strain tensor in the '–' phase, denoted by $\boldsymbol{E}^-$, takes the following form

$$\boldsymbol{E}^- = \begin{bmatrix} 0 & \omega/2 & 0 \\ \omega/2 & 0 & 0 \\ 0 & 0 & 0 \end{bmatrix}. \tag{2}$$

The elastoplastic model of materials for finite deformation proposed by Rice and Hill is adopted in the present paper, see Rice [9, 10] and Hill and Rice [11, 12]. It gives the response between the second Piola-Kirchhoff stress rate tensor $\dot{\boldsymbol{T}}$ and the Green strain rate tensor $\dot{\boldsymbol{E}}$ as follows

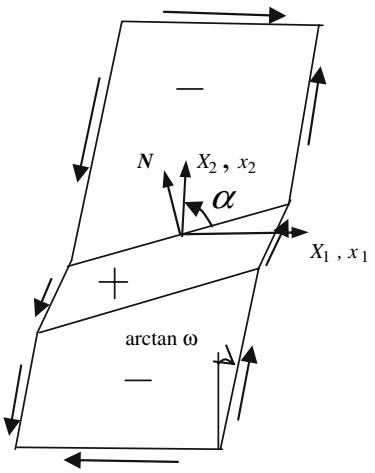

Fig. 1 The top view of a plate under pure shear in the $X_1\,OX_2$ plane

$$\dot{\boldsymbol{T}} = \boldsymbol{L}^{\mathrm{ep}}\dot{\boldsymbol{E}}, \tag{3}$$

where $\boldsymbol{L}^{\mathrm{ep}}$ is the fourth-order elastoplastic stiffness tensor, whose components for the isotropic, linearly hardening J_2-type model take the following form

$$L^{\mathrm{ep}}_{ABCD} = L_{ABCD} - \frac{E^2}{g(1+v)^2}T'_{AB}T'_{CD}, \tag{4}$$

where T'_{AB} are the components of the second Piola-Kirchhoff deviatoric stress tensor $\boldsymbol{T}'$, and $\boldsymbol{T}' = \boldsymbol{T} - \frac{1}{3}(\mathrm{tr}\boldsymbol{T})\boldsymbol{\delta}$, E and v are the elastic modulus and the Poisson ratio of materials, respectively, and the L_{ABCD} are the components of the fourth-order elastic stiffness tensor and are given by

$$L_{ABCD} = 2G\bar{I}_{ABCD} + K\delta_{AB}\delta_{CD} \tag{5}$$

with G being the elastic shear modulus, K the bulk modulus, δ_{ij} the Kronecker delta, and $\bar{I}_{ABCD}$ taking the following form

$$\bar{I}_{ABCD} = \frac{1}{2}(\delta_{AC}\delta_{BD} + \delta_{BC}\delta_{AD}) - \frac{1}{3}\delta_{AB}\delta_{CD}. \tag{6}$$

The g in Eq. 4 takes the form

$$g = \frac{4}{9}E[Y(E^{\mathrm{p}})]^2\left[\frac{E_{\mathrm{p}}}{E} + \frac{3}{2(1+v)}\right], \tag{7}$$

with E_{p} being the plastic modulus defined by

$$E_{\mathrm{p}}(E^{\mathrm{p}}) = \frac{dY(E^{\mathrm{p}})}{dE^{\mathrm{p}}}, \tag{8}$$

and E^{p} being the accumulated plastic deformation and being defined by

$$E^{\mathrm{p}} = \int \dot{E}^{\mathrm{p}}\mathrm{d}t, \tag{9}$$

where t is a time-type variable, and $\dot{E}^{p}$ is the accumulated plastic deformation rate defined by

$$\dot{E}^{\mathrm{p}} = \left[\frac{2}{3}\mathrm{tr}\left[(\dot{\boldsymbol{E}})^{\mathrm{p}}(\dot{\boldsymbol{E}})^{\mathrm{p}}\right]\right]^{1/2} = \left[\frac{2}{3}(\dot{E})^{\mathrm{p}}_{AB}(\dot{E})^{\mathrm{p}}_{AB}\right]^{1/2}. \tag{10}$$

with $(\dot{\boldsymbol{E}})^{\mathrm{p}}$ being the plastic Green strain rate tensor.

The yield criterion in the reference configuration is given by

$$T_{\mathrm{eq}} = Y(E^{\mathrm{p}}), \tag{11}$$

where T_{eq} is the equivalent stress defined by

$$T_{\mathrm{eq}} = \left[\frac{3}{2}\mathrm{tr}(\boldsymbol{T}'\boldsymbol{T}')\right]^{1/2} = \left(\frac{3}{2}T'_{AB}T'_{AB}\right)^{1/2}, \tag{12}$$

and the function $Y(E^{\mathrm{p}})$ describes strain hardening of materials and can be measured by unidirectional tension tests.

It is well known that, for linearly elastic, linearly strain-softening and linearly hardening materials, the plastic modulus E_{p} is related to the elastic modulus E and the tangent modulus E_{t} through

$$\frac{1}{E_{\mathrm{p}}} = \frac{1}{E_{\mathrm{t}}} - \frac{1}{E}. \tag{13}$$

For the '–' phase we have

$$\boldsymbol{T}^{-} = \boldsymbol{L}\boldsymbol{E}^{-} = \begin{bmatrix} 0 & G\omega & 0 \\ G\omega & 0 & 0 \\ 0 & 0 & 0 \end{bmatrix}. \tag{14}$$

A stress–strain response curve with peak stress, sudden dropping and the Maxwell stress plateau was measured in experiments on NiTi alloy strips under uniaxial tension, see, e.g., the curve in the figure 8(b) of Shaw and Kyriakides [5]. The peak stress was regarded as the super yield stress of materials, denoted by $T^{\mathrm{U}}_{\mathrm{y}}$. The lower yield stress, denoted by $T^{\mathrm{L}}_{\mathrm{y}}$, couldn't be measured in experiments, and Shaw and Kyriakides [5] suggested an approximate value for it. Recently Zhang et al. [8] proposed a method to determine the value theoretically. For the pure shear defined by Eq. 1, the super yield stress tensor and the lower yield stress tensor, denoted by $\boldsymbol{T}_{\mathrm{yU}}$ and $\boldsymbol{T}_{\mathrm{yL}}$, respectively, take the following forms

$$\begin{aligned} \boldsymbol{T}^{\mathrm{yU}} &= \begin{bmatrix} 0 & T_{\mathrm{yU}}/\sqrt{3} & 0 \\ T_{\mathrm{yU}}/\sqrt{3} & 0 & 0 \\ 0 & 0 & 0 \end{bmatrix}, \\ \boldsymbol{T}^{\mathrm{yL}} &= \begin{bmatrix} 0 & T_{\mathrm{yL}}/\sqrt{3} & 0 \\ T_{\mathrm{yL}}/\sqrt{3} & 0 & 0 \\ 0 & 0 & 0 \end{bmatrix} \end{aligned} \tag{15}$$

For linearly hardening materials, the stress inside the '+' phase can be given by

$$\boldsymbol{T}^{+} = \boldsymbol{T}^{\mathrm{yL}} + \dot{\boldsymbol{T}}. \tag{16}$$

Analysis of two-phase equilibrium under plane shear

Governing equations

Multi-phase equilibrium requires that the following equilibrium equations away from interfaces between phases must be satisfied (in the absence of body forces)

$$\mathrm{Div}\boldsymbol{\pi}^T = \mathbf{0}, \tag{17}$$

where Div is the divergence operator in the reference configuration, $\boldsymbol{\pi}$ is the first Piola-Kirchhoff stress tensor, and the superscript T signifies the transpose of tensors.

The stress across interfaces between phases is generally discontinuous, i.e. in general,

$$\pi_{iA}^{+} \neq \pi_{iA}^{-}. \tag{18}$$

For a continuum the continuity of traction across interfaces must be satisfied, namely

$$[\boldsymbol{\pi}]\boldsymbol{N} = \mathbf{0}, \tag{19}$$

where $[g] = g^{+}-g^{-}$ is defined as a jump of the function g across an interface that divided the body into two phases.

In order to satisfy the continuity of displacements across interfaces the jump $[\boldsymbol{F}]$ must necessarily take the form, see Fu and Freidin [13],

$$[\boldsymbol{F}] = \boldsymbol{f} \otimes \boldsymbol{N}. \tag{20}$$

where $\boldsymbol{f}$ is a vector. From (20) $\boldsymbol{f}$ can be written as

$$\boldsymbol{f} = [\boldsymbol{F}]\boldsymbol{N}. \tag{21}$$

For phase transformations the following Maxwell relation must be satisfied,

$$[W] - \boldsymbol{f} \cdot \boldsymbol{\pi}\boldsymbol{N} = 0, \tag{22}$$

where $W$is the stress-work function that satisfies

$$\frac{\partial W(\boldsymbol{E})}{\partial E_{AB}} = T_{AB} \tag{23}$$

with T_{AB} and E_{AB} being the components of the second Piola-Kirchhoff stress tensor $\boldsymbol{T}$ and the Green strain tensor $\boldsymbol{E}$, respectively.

The Maxwell relation represents the continuity of the Eshelby traction across interfaces, see Gurtin [14]. The importance of the Maxwell relation was first noted by Ericksen [15], Grinfeld [16] and Abeyaratne [17], but it was Fredin and Chiskis [18, 19] who first used it as an equilibrium condition in characterizing multi-phase deformations. Recently, this approach has been used by Fu and Zhang [20] in characterizing kink-band formation in fibre-reinforced composites and by Zhang et al. [8] in the elastoplastic modeling of materials supporting multiphase deformations.

For piecewise-homogenous deformations, the equilibrium equations are trivially satisfied. Two-phase equilibrium can occur only if the jump conditions (19) and (22) are satisfied. Equations 19 and 22 are the governing equations for two-phase piecewise-homogeneous deformations.

The stress inside the '–' phase

From Eq. 14 and $\boldsymbol{\pi} = \boldsymbol{FT}$, the first Piola-Kirchhoff stress tensor inside the '–' phase can be written as

$$\boldsymbol{\pi}^{-} = \begin{bmatrix} T_{12}^{-}\omega & T_{12}^{-} & 0 \\ T_{12}^{-}\lambda_2 & 0 & 0 \\ 0 & 0 & 0 \end{bmatrix}, \tag{24}$$

and the strain energy is given by

$$W^{-} = (T_{12}^{-})^2/2G. \tag{25}$$

The strain and stress inside the '+' phase

For the pure shear deformation in the $X_1\,OX_2$ plane we can assume that the $\boldsymbol{N}$and the $\boldsymbol{f}$ take respectively the forms

$$\boldsymbol{N} = [N_1, N_2, 0]^T, \tag{26}$$

$$\boldsymbol{f} = [f_1, f_2, 0]^T, \tag{27}$$

So we have

$$[\boldsymbol{F}] = \begin{bmatrix} f_1N_1 & f_1N_2 & 0 \\ f_2N_1 & f_2N_2 & 0 \\ 0 & 0 & 0 \end{bmatrix}. \tag{28}$$

Consequently we have $\boldsymbol{F}^{+} = \boldsymbol{F}^{-} + [\boldsymbol{F}], \boldsymbol{E}^{+} = \frac{1}{2}(\boldsymbol{F}_{+}^{T}\boldsymbol{F}_{+} - \boldsymbol{I})$, and

$$\dot{\boldsymbol{E}} = \boldsymbol{E}^{+} - \boldsymbol{E}^{yL}. \tag{29}$$

Substituting (29) into (3) gives $\dot{\boldsymbol{T}}$, and then from (16) the $\boldsymbol{T}^{+}$ can be determined. So the jump of stress tensor across interfaces is obtained through

$$[\boldsymbol{\pi}] = \boldsymbol{F}^{+}\boldsymbol{T}^{+} - \boldsymbol{\pi}^{-}. \tag{30}$$

The stress-work function for the '+' phase is given by $W^{+} = \int_0^{E_{AB}^{+}} T_{AB}^{+}(\boldsymbol{E}^{+})dE_{AB}^{+}$. In particular, for trilinear stress-strain response (linear elasticity, linearly strain-softening, linearly hardening), we have

$$\begin{aligned} W^{+} = &\frac{1}{2}T_{AB}^{yU}E_{AB}^{yU} + \frac{1}{2}(T_{AB}^{yU} + T_{AB}^{yL})(E_{AB}^{yL} - E_{AB}^{yU}) \\ &+ T_{AB}^{yL}\dot{E}_{AB} + \frac{1}{2}\dot{T}_{AB}\dot{E}_{AB}. \end{aligned} \tag{31}$$

Jump conditions for two-phase piecewise-homogenous deformations

Substituting (26) and (30) into (19), and (24–28) into the Maxwell relation (22) give the following three equations

$$q_1(T_{12}^-, f_1, f_2, N_1, N_2) = 0, \tag{32}$$

$$q_2(T_{12}^-, f_1, f_2, N_1, N_2) = 0, \tag{33}$$

$$q_3(T_{12}^-, f_1, f_2, N_1, N_2) = 0. \tag{34}$$

The analysis of stress-induced phase transformation is reduced to finding the minimum value of T_{12}^- that makes Eqs. 32–34 together with $N_1^2 + N_2^2 = 1$ have a unique, real, physically acceptable solution for $[f_1, f_2, N_1, N_2]^{\mathrm{T}}$. The physically acceptability means that for the plate under pure shear shown in Fig. 1, where $N_2 > 0$, the real solution must satisfy $f_1 > 0$ in order to ensure that $[\, F_{12} \,] > 0$, in other words, the material inside the '+' phase should be further sheared.

Equations 32–34 are strongly non-linear. In the following section, we consider their numerical solutions.

Numerical illustration

As a numerical illustration, a stress–strain response curve under uniaxial tension measured in experiments on NiTi alloy strips by Shaw and Kyriakides [5] is adopted in this paper to calibrate the three-dimensional elastoplastic model, see the curve of the nominal stress against the Engineering strain in the figure 8 (b) by Shaw and Kyriakides [5]. For the convenience of reading, the curve is sketched in Fig. 2 in broad line, where S is the nominal stress, and $\gamma = \lambda - 1$ is the engineering strain with λ being the stretch in the tension direction.

The peak stress is usually chosen as the supper yield stress, and from the curve by Shaw and Kyriakides [5] we have the values of stress and strain at supper yield point:

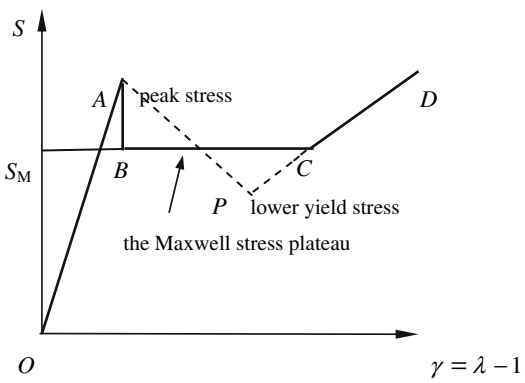

Fig. 2 A typical strain–stress response curve of NiTi alloy under uniaxial tension

$S_y^U = 403$ Mpa and $\gamma_y^U = 0.0065$. It is difficult to measure the lower yield stress S_y^L in experiments, and the values of the stress and strain at lower yield point were given approximately in Shaw and Kyriakides [5]. In the present paper, using the method suggested by Zhang et al. [8], the values can be determined theoretically, and it is given that $S_y^L = 386$ MPa and $\gamma_y^L = 0.046$. The corresponding values of the second Piola-Kirchhoff stress, the Green strain and the elastic and hardening moduli of the material can be easily evaluated from the above values: $T_y^U = 400.397$ MPa and $E_y^U = 0.00652112$ at the upper yield point, $T_y^L = 368.321$ MPa and $E_y^L = 0.049152$ at the lower yield point, the elastic modulus $E = 61400.1$ MPa, and the hardening modulus (tangent modulus) $E_t = 38624.8$ MPa, respectively. The Poisson ratio takes the value of 0.3 in the present analysis.

After the calibration above, Eqs. 32–34 are still very involved. With the aid of PHC (Polynomial Homotopy Continuation) software package, numerically solving Eqs. 34–36 together with $N_1^2 + N_2^2 = 1$ shows that:

1. If $[f_1, f_2, N_1, N_2\,]^{\mathrm{T}}$is a real solution $[-f_1, -f_2, -N_1, -N_2]^{\mathrm{T}}$ is a real solution too. Namely, the number of the real solutions is always a multiple of two. Since $[-N_1, -N_2]^{\mathrm{T}}$ signifies the unit vector that is normal to the other interface in Fig. 1 and points from the '+' phase into the '–' phase, only the solutions in which $N_2 > 0$ and $f_1 > 0$ are concerned in the following analysis.
2. When $T_{12}^- = 221.072731$ there are four real solutions for $[f_1, f_2, N_1, N_2\,]^{\mathrm{T}}$ in which $N_2 > 0$ and $f_1 > 0$ as follows

$$\begin{Bmatrix} f_1 \\ f_2 \\ N_1 \\ N_2 \end{Bmatrix} = \begin{Bmatrix} 6.50267527636302\mathrm{E}{-02} \\ -2.72684603738399\mathrm{E}{-03} \\ 1.05568143303551\mathrm{E}{-06} \\ 9.99999999999443\mathrm{E}{-01} \end{Bmatrix}, \tag{35}$$

$$\begin{Bmatrix} f_1 \\ f_2 \\ N_1 \\ N_2 \end{Bmatrix} = \begin{Bmatrix} 6.50432903280873\mathrm{E}{-02} \\ -2.54458599200413\mathrm{E}{-03} \\ -6.56671569459601\mathrm{E}{-03} \\ 9.99978438890052\mathrm{E}{-01} \end{Bmatrix}, \tag{36}$$

$$\begin{Bmatrix} f_1 \\ f_2 \\ N_1 \\ N_2 \end{Bmatrix} = \begin{Bmatrix} 6.50267549327202\mathrm{E}{-02} \\ -1.99718554592573\mathrm{E}{+00} \\ 1.12011039838613\mathrm{E}{-09} \\ 1.00000000000000\mathrm{E}{+00} \end{Bmatrix}, \tag{37}$$

$$\begin{Bmatrix} f_1 \\ f_2 \\ N_1 \\ N_2 \end{Bmatrix} = \begin{Bmatrix} 6.56671569459013\mathrm{E}{-03} \\ 1.93557966369579\mathrm{E}{-03} \\ -6.50642610496734\mathrm{E}{-02} \\ -9.99978438890052\mathrm{E}{-01} \end{Bmatrix}. \tag{38}$$

Subtituting the solution (35) into Eq. 28 gives $[\boldsymbol{F}]$. Then we have consequently $\boldsymbol{F}^+ = \boldsymbol{F}^- + [\boldsymbol{F}]$ and

$\boldsymbol{U}_+^2 = (\boldsymbol{F}^+)^{\mathrm{T}}\boldsymbol{F}^+$ (where $\boldsymbol{U}$ is the right strecth tensor). With the aid of Mathematica or Maple, it is easy to find that the eigenvalues (principal streches) of the $\boldsymbol{U}_+$ are (1.03653, 1., 0.962087), and the corresponding eigenvectors are $[0.707107, 0.707106, 0.]^{\mathrm{T}}$, $[0., 0., 1.]^{\mathrm{T}}$ and $[-0.707106, 0.707107, 0.]^{\mathrm{T}}$, respectively. As the three principal stretches are all greater then zero the solution (32) is physically acceptable.

Following the same procedure above, we find that, for each of the solutions (36), (37) and (38), there is always one of the eigenvalues of $\boldsymbol{U}_+$ that is less than zero, so that the solutions (36), (37) and (38) are not phyysically acceptable.

3. When $T_{12}^- = 221.072730$ there is no real solution for $[f_1, f_2, N_1, N_2]^{\mathrm{T}}$ in which $N_2 > 0$ and $f_1 > 0$.

Finally, we obtain a unique, real, physically acceptable solution (35) with

$$(T_{12}^-)_{\min} = 221.0727304(\mathrm{MPa}). \tag{39}$$

More than 6 significant figures are used in the equations above to show the calculating precision. In the following equations only 6 significant figures are used. Furthermore, values of order 10^{-6}, or smaller, will be reported as zero due to round off.

The deformation gradients inside the A- and M-phases are given, respectively, by

$$\boldsymbol{F}^- = \begin{bmatrix} 1. & 0.936138\times10^{-2} & 0 \\ 0.0239440 & 0.999956 & 0 \\ 0 & 0 & 1 \end{bmatrix}, \tag{40}$$

$$\boldsymbol{F}^+ = \begin{bmatrix} 1. & 0.0743881 & 0 \\ 0.0 & 0.997229 & 0 \\ 0 & 0 & 1 \end{bmatrix}. \tag{41}$$

The jump of the deformation gradient across the interface is given by

$$[\boldsymbol{F}] = \begin{bmatrix} 0.0 & 0.0650268 & 0 \\ 0.0 & -0.272685\times10^{-2} & 0 \\ 0 & 0 & 0 \end{bmatrix}. \tag{42}$$

The stress inside the A-phase, i.e. the Maxwell stress, is given by

$$\boldsymbol{T}^- = \begin{bmatrix} 0 & 221.073 & 0 \\ 221.073 & 0 & 0 \\ 0 & 0 & 0 \end{bmatrix}(\mathrm{MPa}), \tag{43}$$

and the stress inside the M phase takes the form

$$\boldsymbol{T}^+ = \begin{bmatrix} 0.463237\times10^{-2} & 221.073 & 0 \\ 221.073 & 0.0 & 0 \\ 0 & 0 & 0.13901\times10^{-2} \end{bmatrix} \times (\mathrm{MPa}). \tag{44}$$

Since the upper and lower surfaces of the '+' phase are stress free there must be $T_{33}^+ = 0$ inside the '+' phase. But from Eq. 44 we have $T_{33}^+ = 0.13901\times10^{-2}$ MPa although the value of T_{33}^+ is very small as compared to the value of T_{12}^+. In order to ensure that

$$T_{33}^+ = 0, \tag{45}$$

inside the '+' phase, Eq. 28 is replaced by

$$[\boldsymbol{F}] = \begin{bmatrix} f_1N_1 & f_1N_2 & 0 \\ f_2N_1 & f_2N_2 & 0 \\ 0 & 0 & \lambda_3^+ - 1 \end{bmatrix}, \tag{46}$$

where λ_3^+ is the stretch in the thickness direction of the plate in the '+' phase. Following the similar procedure to the one described in Section "Analysis of two-phase equilibrium under plane shear", the three equations similar to Eqs. 32–34 but with λ_3^+ included are obtained as follows

$$s_1(T_{12}^-, f_1, f_2, N_1, N_2, \lambda_3^+) = 0, \tag{47}$$

$$s_2(T_{12}^-, f_1, f_2, N_1, N_2, \lambda_3^+) = 0, \tag{48}$$

$$s_3(T_{12}^-, f_1, f_2, N_1, N_2, \lambda_3^+) = 0. \tag{49}$$

Solving Eqs. 45, 47–49 together with $N_1^2 + N_2^2 = 1$ gives a unique, real, physically acceptable solution

$$\begin{Bmatrix} f_1 \\ f_2 \\ N_1 \\ N_2 \\ \lambda_3^+ \end{Bmatrix} = \begin{Bmatrix} 6.50268\mathrm{E}\text{-}02 \\ -2.72684\mathrm{E}\text{-}03 \\ 0.0 \\ 1.00000 \\ 1.00000 \end{Bmatrix} \tag{50}$$

with $(T_{12}^-)_{\min} = 221.073$ Mpa.

Comparing the solution above with the solution (35) shows that the values of the two solutions are very close, but the solution (50) will give the more precise value of the stress inside the '+' phase.

The corresponding Maxwell stress $\boldsymbol{T}^-$ is then given by

$$\boldsymbol{T}^- = \begin{bmatrix} 0 & 221.073 & 0 \\ 221.073 & 0 & 0 \\ 0 & 0 & 0 \end{bmatrix}(\mathrm{MPa}), \tag{51}$$

and the stress inside the '+' phases is in the form

$$\boldsymbol{T}^{+} = \begin{bmatrix} 0.421593 \times 10^{-2} & 221.073 & 0 \\ 221.073 & 0 & 0 \\ 0 & 0 & 0.0 \end{bmatrix} (\text{MPa}). \quad (52)$$

The inclination angle of the '+' phase band to the X_2-axis is given by $\alpha = 90°–\tan^{-1}(–N_1/N_2)$. We have

$$\alpha = 90.0°,$$

i.e. a locally deformed '+' phase band can coexist with the '–' phase in plates under plane shear and the band is perpendicular to the X_2-axis.

It is difficult to carry out experiments on plates under plane shear. Experiments on thin-walled NiTi alloy tubes under torsion were carried out by Sun and Li [4], where no locally deformed M-bands were observed. The above predicted value of $\alpha = 90.0°$ can be used to explain the observation.

Thin-walled NiTi alloy tube under torsion

A thin-walled NiTi alloy tube under torsion with a possible spiral M-band is plotted in Fig. 3. The $X_1(x_1)$-axis is parallel to the cross section of the tube, the $X_2(x_2)$-axis and the $X_3(x_3)$-axis are along the axis of the tube and the thickness direction of the tube, respectively. The unit vector that is normal to the A–M interface in the reference configuration and points from the M-phase into the A-phase is denoted also by $\boldsymbol{N} = [N_1, N_2, N_3]^{\mathrm{T}}$ as shown in Fig. 1.

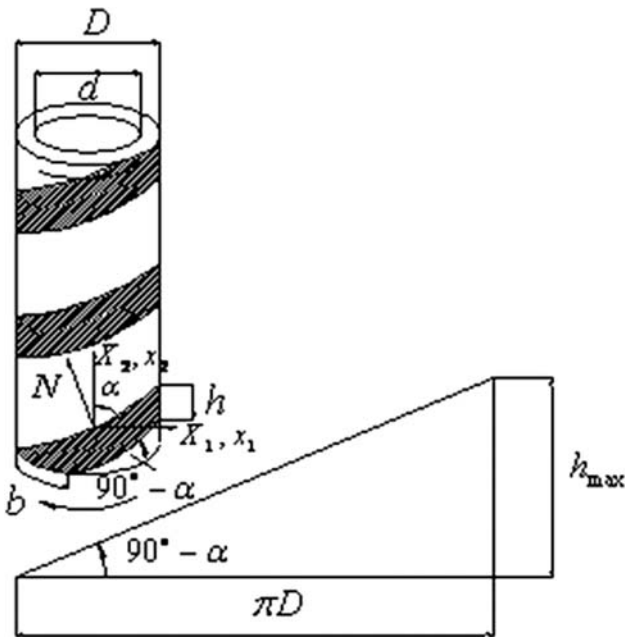

Fig. 3 A thin-walled tube under torsion

For a thin-walled tube it can be assumed that the stress along the thickness direction of the tube is homogeneous, so every material particle of the tube is under pure shear in the $X_1\,OX_2$ plane as the particle in the plate is. It is worth noting that the possible inclined '+' phase band in the plate shown in Fig. 1 becomes a spiral M-band (the shadowed band in Fig.3) on the tube, and its spiral angle is equal to $90°–\alpha$ as shown in Fig. 3.

Two distinct observations were found in the experiments on NiTi alloy thin-walled tubes under tension and torsion, respectively. A spiral M-band on the tube under axial tension was observed. The M-band initiated at a peak stress, and then, following a sudden drop of stress, spread along the length direction of the tube under an approximately constant stress (the Maxwell stress plateau) until the whole tube transformed into the M-phase. When NiTi tubes were subjected to torsion, however, no locally deformed spiral M-band on tubes was observed, and the austenite phase was transformed into the M-phase homogeneously throughout whole tubes when the applied toque reached a critical value. I addition no Maxwell plateau was observed.

From Fig. 3, the height and the maximal height of the possible spiral M-band, denoted by h and $h_{\max}$, are given respectively by $h = b\,\tan|90°–\alpha|$ and $h_{\max} = \pi\,D\,\tan|90°–\alpha|$, where b is the arc length of the section of the periphery of the end-face of the tube where the spiral M-band initiates from, and D is the outer diameter of the tube. For the tube under tension along its axial direction, with the aid of the method suggested in Zhang et al. [8], the inclination angle of the M-band to the axis of the tube can be predicted, and the predicted value of 61.05° for α is very close to the measured value of 61° by Sun and Li [4]. For this inclination angle value of 61° the maximal height of the spiral M-band is given by $h_{\max} = \pi\,D\tan 29° \approx 1.741D$, so that under tension the spiral M-band can spreads from $h = 0$ to $h = 1.741D$, and when $h = 1.741D$ the whole tube transformed into the M-phase.

For the tube under torsion, the predicted value of the inclination angle of the M-band is 90°, and the maximal height of the possible M-band is given by $h_{\max} = 0$, so that the spreading of the M-band cannot occur, and the localized deformed M-band and the Maxwell plateau cannot be observed in experiments..

Conclusions

The stress-induced phase transformation in elastoplastic materials with strain-softening behavior under plane shear is investigated. Discontinuities of stress and deformation gradient across interfaces between phases are considered, and continuity of traction and displacement across interfaces and the Maxwell relation are imposed. The governing

equations are obtained. The analysis is reduced to finding the minimum value of the loading at which governing equations have a unique, real, physically acceptable solution. The following conclusions can be drawn out.

- Stress-induced phase transformations can occur in elastoplastic materials with strain-softening behavior under plane shear. A unique physically acceptable solution can be obtained. The Maxwell stress, the jumps of stress and deformation gradient across the interface and the inclination angle of the locally deformed band can all be determined.
- For the plate under plane shear two-phase piecewise-homogeneous deformations can coexist, and the inclination angle of the locally deformed band to the X_2-axis is 90°.
- The predicted value of inclination angle of M-band, 90°, can be applied to explain why no spiral M-band and the Maxwell stress plateau were observed in experiments on thin-walled NiTi alloy tubes under torsion.

Acknowledgements This research is supported by a joint grant from the National Nature Science Foundation of China and the Royal Society UK under their Joint Project Scheme and another grant from the National Nature Science Foundation of China under Project No. 10272079. We are also grateful to Professor F.S. Bai for the help on homotopy continuation methods.

References

1. Wattrisse B, Chrysochoos A, Muracciole J-M, Némoz-Gaillard M (2001) Eur J Mech A/Solids 20:189
2. Corona E, Shaw JA, Iadicola MA (2002) Int J Solid Struct 39:3313
3. Shaw JA, Kyriakides S (1997) Acta Materialia 45:683
4. Sun QP, Li ZQ (2002) Int J Solid Struct 39:3797
5. Shaw JA, Kyriakides S (1998) Int J Plasticity 13(10):837
6. Kyriakides S, Miller JE (2000) ASME J Appl Mech 67:645
7. Sun HB, Yoshida F, Ma X, Kameia T, Ohmori M (2003) Mater Lett 57:3206
8. Zhang YT, Ren SG, Ao T (2007) Mater Sci Eng A 447:332
9. Rice JR (1971) J Mech Phys Solids 19:433
10. Rice JR (1975) In: Argon AS (ed) Constitutive equations in plasticity [C]. MIT Press, New York, pp. 23–79
11. Hill R, Rice JR (1972) J Mech Phys Solid 20:401
12. Hill R, Rice JR (1973) SIAM J Appl Math 25(3):448
13. Fu YB, Freidin AB (2004) Proc R Soc Lond A 460:3065
14. Gurtin ME (2000) Configurational forces as basic concepts of continuum physics. Springer, New York
15. Ericksen JL (1975) J Elasticity 5(1):191
16. Grinfeld MA (1980) Dokl Akad Nauk SSSR 251:824
17. Abeyaratne R (1983) J Elast 13:175
18. Freidin AB, Chiskis AM (1994) Izv Ran Mekhanika Tverdogo Tela (Mechanics of Solids) 29:91
19. Freidin AB, Chiskis AM (1994) Izv Ran Mekhanika Tverdogo Tela (Mechanics of Solids) 29:46
20. Fu YB, Zhang YT (2006) Int J Solid Struct 43:3306